Macromolecules

Article

pubs.acs.org/Macromolecules

Syndiotactic Polyallyltrimethylsilane-Based Stereoregular Diblock Copolymers: Syntheses and Self-Assembled Nanostructures

Jing-Yu Lee, Min-Ching Shiao, Fu-Yuan Tzeng, Chin-Hung Chang, Chih-Kuang Tsai, and Jing-Cherng Tsai*

Department of Chemical Engineering, National Chung Cheng University, Chia-Yi 62142, Taiwan

Kuan-Hsin Lo, Shih-Chieh Lin, and Rong-Ming Ho*

Department of Chemical Engineering, National Tsing Hua University, Hsinchu 30013, Taiwan

Supporting Information

ABSTRACT: Structurally well-defined stereoregular diblock copolymers composed of syndiotactic polyallyltrimethylsilane (sPATMS) and poly(methyl methacrylate) (PMMA) were prepared by using an α-bromoester-terminated sPATMS macroinitiator, which was chain extended by MMA using a cuprous halide-based atom transfer radical polymerization (ATRP) system. The α-bromoester-terminated sPATMS macroinitiator was prepared via the esterfication of hydroxyl-capped sPATMS with α-bromoisobutyryl bromide. The hydroxyl-capped sPATMS was generated via a selective chain transfer reaction to triethylaluminum (TEA) during the syndiospecific polymerization of allyltrimethylsilane (ATMS) conducted in the presence of syndiospecific *ansa*-metallocene catalysts. The proposed synthetic route not only offers the high-yield production of stereoregular sPATMS-*b*-PMMA but also provides the linking of the stereoregular block (sPATMS) with PMMA through a controlled/living radical polymerization process. Moreover, the proposed method offers effective control over the block chain length, the molecular weight distribution (M_w/M_n) and the stereoregularity of sPATMS block. Thus, the self-assembly of the resultant diblock copolymers produces well-ordered nanostructures from microphase separation, as evidenced by transmission electron microscopy and small-angle X-ray scattering results.

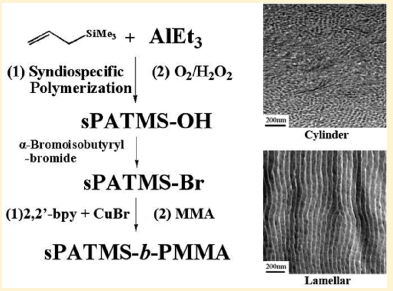

INTRODUCTION

Self-assembly is the spontaneous association of compounds under equilibrium conditions into stable, structurally well-defined aggregates via cooperating secondary interactions (namely, noncovalent bonding forces) without human intervention.[1,2] The self-assembly of synthetic molecules, especially block copolymers (BCPs), have been comprehensively studied for their fascinating phase behaviors and tunable properties.[3] Block copolymers consist of chemically distinct polymer chains covalently linked to form a single molecule. Owing to their mutual repulsion, dissimilar blocks tend to segregate into different domains so as to self-assemble into one-, two-, or three-dimensional periodic nanostructures in the bulk state.[4] In the simplest case of noncrystalline flexible coiled diblock copolymers, various nanostructures such as spheres (S), cylinders (C), gyroid (G), and lamellae (L) can be found, depending on the relative compositions (i.e., volume fraction) between blocks, the sequence of constituted blocks and the architecture of polymer chains as well as the persistence lengths of blocks. In contrast to the formation of conventional phases from the self-assembly of noncrystalline BCPs, the competition between crystallization and microphase separation in the self-assembly of semicrystalline BCPs has attracted extensive attention because the crystallization will affect the self-assembled nanostructures and create various interesting morphologies.[5] Namely, the final morphology of semicrystalline BCPs is strongly dependent upon the experimental temperature, with respect to the order−disorder transition temperature (T_{ODT}), the crystallization temperature of the crystalline block (T_c^c), the glass transition of the amorphous block (T_g^a), and the crystallization rate.[6] As a result, well-defined nanostructures can thus be tailored by the molecular engineering of synthetic BCPs, which provides promising features for the applications of nanotechnologies.[7,8]

Silicon-containing polymers have attracted growing interests as functional materials due to their unique physical properties, including high oxygen permeability, low surface energy, high electrical resistance (insulator), thermal stability, photostability, and ease of cross-linking.[9] For the formation of self-assembled nanostructures, in particular nanostructured thin films, silicon-containing BCPs have been demonstrated to function as rigid nanopatterned templates that can be used for pattern transfer in nanoimprint lithography.[10] Despite this, studies on the self-assembly of silicon-containing BCPs have been quite limited due to the difficulty in the preparation of structurally well-defined silicon-containing BCPs.[11,12] This limits the preparation of silicon-containing BCPs for use in self-assembling studies and hampers their use in nanotechnological applications.

Received: January 5, 2012
Revised: February 28, 2012
Published: March 13, 2012

We have previously conducted syntheses and self-assembling studies of propylene- and styrene-based stereoregular diblock copolymers.[13] Previous studies have demonstrated that the incorporation of stereoregular and crystallizable moieties within block copolymers enhances morphological richness and offers various morphological controls in the self-assembly processes.[14,15] The prospect of using silicon-containing stereoregular BCPs for their self-assembly studies and for use as rigid nanopatterned templates have prompted us to develop a method for their preparation, which is unable to achieve using existing methods.

Stereoregular silicon-containing polymers, including isotactic polyallytrimethylsilane (iPATMS) and syndiotactic polyallytrimethylsilane (sPATMS), have been prepared via stereospecific polymerization of allytrimethylsilane using Zieglar−Natta[16] and metallocene catalysts,[17] respectively. Nevertheless, the syntheses of stereoregular silicon-containing BCPs remain a synthetic challenge. How to achieve the connection between the silicon-containing stereoregular block and the other polymer block with high linking efficiency is essential in addition to accomplish the block length control in the construction of silicon-containing stereoregular BCPs. Methods for syntheses of α-olefin-based stereoregular BCPs with simultaneous stereoregularity, block connection and block length controls via stereospecific living polymerization of various α-olefins have been developed using stereospecific living coordination catalysts[18] or stereospecific controlled/living radical polymerization catalysts.[19] Unfortunately, silicon-containing stereoregular BCPs cannot be synthesized directly by using these stereospecific living polymerization systems as silicon-containing α-olefins (e.g., allytrimethylsilane) fail to undergo the respective stereospecific living polymerization reactions.

Another approach for the construction of silicon containing stereoregular BCPs is to conduct a selective chain transfer reaction during stereospecific polymerization of silyl group-containing α-olefins for the generation of an end-functionalized silyl group-containing stereoregular prepolymer in the first step, and then use the end-functionalized prepolymer in postpolymerization reaction for block formation. This two-step process allows for a broad variety of polymer architecture linked onto the silicon-containing stereoregular block but it needs to overcome the difficulty in the synthesis of silyl group-containing end-functionalized stereoregular prepolymer, which can only be generated via the induction of a selective chain transfer reaction during stereospecific polymerization of silyl group-containing α-olefins.[20]

Herein, silicon-containing stereoregular BCPs composed of syndiotactic polyallyltrimethylsilane (sPATMS) and poly(methyl methacrylate) (PMMA) are prepared by using an α-bromoester-terminated sPATMS macroinitiator, which is chain extended by MMA via the controlled/living radical polymerization of MMA using a cuprous halide-based ATRP process. The α-bromoester-terminated sPATMS macroinitiator is prepared via the esterfication of hydroxyl-capped sPATMS with α-bromoisobutyryl bromide. The hydroxyl-capped sPATMS can be generated by inducing a selective chain transfer reaction to triethylaluminum (TEA) during the syndiospecific polymerization of allyltrimethylsilane (ATMS) conducted in the presence of syndiospecific *ansa*-metallocene catalysts. The unique synthetic route allows the preparation of structurally well-defined silyl-containing stereoregular BCPs with good yield. The obtained silyl-containing stereoregular BCPs give a uniform chemical architecture and can self-assemble into well-ordered nanostructures, as evidenced by transmission electron microscopy (TEM) and small-angle X-ray scattering (SAXS) results.

EXPERIMENTAL SECTION

General Procedure. All reactions and manipulations were conducted under a nitrogen atmosphere using the standard Schlenk line or drybox techniques. Solvents and common reagents were commercially obtained and used either as received or purified by distillation with sodium/benzophenone. Allyltrimethylsilane (ATMS, purity >98%) and methyl methacrylate (99%) purchased from Aldrich were dried over calcium hydride and distilled under vacuum before use. Oxygen (purity >99.5%) was obtained from Matheson and were used as received. $Me_2C(Cp)(Flu)ZrCl_2$ (**I**)[21] and $Ph_2Si(Cp)(Flu)ZrCl_2$ (**II**)[22] were synthesized using methods described in the literature. The α-bromoisobutyryl bromide (98%), copper bromide (98%) and 1,10-phenanthroline (>99%) were purchased from Aldrich and used as received. Triethylaluminum (TEA, 1 M in hexane) was purchased from Aldrich and used as received. Methylaluminoxane (MAO, 14% in toluene), purchased from Albemarle, was dried under vacuum to remove residual TMA.[23] The resulting TMA-free MAO was diluted in toluene to the desired concentration before use.

Preparation of Hydroxyl-Capped sPATMS. Representative experiment (for entry 11 of Table 1): A 100 mL stainless steel reactor, equipped with a magnetic stirrer, was allowed to dry at 80 °C under vacuum. After being refilled with nitrogen, the reactor was cooled to −20 °C and then charged sequentially with 20 mL of toluene, 25.0 mmol of MAO, and 12.5 μmol of $Me_2C(Cp)(Flu)ZrCl_2$. After the reactor was allowed to stir at −20 °C for 5 min, it was charged with 8.0 mmol of TEA and then with 31.5 mmol ATMS to initiate the polymerization reaction. Polymerization was conducted at −20 °C for 24 h. The polymer solution was then treated with oxygen at a flow rate of 10 mL/min for 1 h. The solution was slowly warmed to room temperature and was then charged with H_2O_2 (5 mL, 30% in H_2O). After being stirred at room temperature for 30 min, the solution was charged with excess methanol (ca. 40 mL), which led to the deposition of the OH-capped sPATMS as a white precipitate. After isolation by filtration, the resulting polymer was purified by removing the atactic polyallytrimethylsilane via boiling acetone extraction in a Soxhlet extractor. The resulting insoluble fraction of the polymer was dried under vacuum to provide 1.64 g of OH-capped sPATMS [M_n = 15800, M_w/M_n = 1.81 by GPC (in THF at 40 °C)].

Fractionation of Hydroxyl-Capped sPATMS. On a vacuum line, 0.7 g of OH-capped sPATMS (M_n = 15800, M_w/M_n = 1.81, entry 11 of Table 1) was placed in a Soxhlet extractor and allowed to undergo Soxhlet extraction in a boiling MEK/THF mixture (5:1) for 24 h. The resulting MEK/THF solution was collected and allowed to concentrate under vacuum to 10 mL. The resulting solution was then charged with excess methanol (ca. 20 mL), which resulted in the deposition of a MEK/THF-soluble OH-capped sPATMS sample as a white precipitate. The resulting precipitate was isolated by filtration and dried under vacuum to provide 0.53 g of OH-capped sPATMS [M_n = 13300, M_w/M_n = 1.40 by GPC (in THF at 40 °C)].

Preparation of α-Bromoisobutylester-Capped sPATMS. In a 200 mL round-bottom flask, 0.35 g of OH-capped sPATMS (M_n= 13300, M_w/M_n= 1.40) was allowed to dissolve in 50 mL of toluene. The solution was then charged with excess Et_3N (ca., 1.0 mL) and then with excess α-bromoisobutyryl bromide (ca. 0.5 mL). The resulting solution was allowed to heat up to 60 °C; the esterfication reaction was conducted at 60 °C for 4 h. The reaction solution was cooled to room temperature and then charged with excess methanol (~80 mL), which led to the deposition of a sPATMS-based polymer as a pale brown precipitate. The resulting reaction product was collected through filtration, washed with methanol, and dried under high vacuum to provide 0.34 g of α-bromoisobutylester-capped sPATMS [M_n = 13500, M_w/M_n = 1.40 by GPC (in THF at 40 °C)].

Synthesis of sPATMS-*b*-PMMA. In a drybox, a 100 mL Schlenk flask equipped with a magnetic stirrer was charged sequentially with 0.26 g (0.02 mmol) of α-bromoisobutylester-capped sPATMS (M_n = 13500, M_w/M_n = 1.4), 30 mL of toluene, 5.5 μmol of copper bromide, and then 11.0 μmol of 1,10-phenanthroline.[24] The reaction vessel was capped and removed from the drybox. The reaction vessel was immersed in a oil bath and was allowed to heat up to 95 °C for 30 min for the in situ

Table 1. Preparation of End-Functionalized Stereoregular Polyallyltrimethylsilane via Selective ChainTransfer to Triethylaluminum (TEA) Mediated by Various Syndiospecific Metallocene Catalysts[h]

run	catal[a]	chain transfer agent	alkylaluminum (mmol)	temp (°C)	activity[c]	M_n[d]	PDI[d]	M_n[e] (calcd)	T_m[f] (°C)	$-\Delta H$[f] (J/g)	end group ratio(%)[g] hydroxyl	vinylidene
1	I	TEA[b]	2	20	13.03	9800	1.74	6100	250	10.6	31.4	68.6
2	I	TEA	4	20	10.51	7200	1.77	4500	248	8.5	39.4	61.6
3	I	TEA	6	20	8.47	4800	1.66	2800	244	5.6	45.4	54.6
4	I	TEA	8	20	6.24	4600	1.54	2500	238	4.4	49.2	51.8
5	I	TEA	8	40	18.42	2100	1.31	1200	250	2.8	42.8	57.2
6	I	TEA	8	0	7.72	14 800	1.70	11 200	255	18.6	63.4	36.6
7	I	TMA	8	0	4.65	16 200	1.86	13 100	249	16.7	58.4	41.8
8	I	TEA	2	−20	14.14	57 700	2.04	32 300	263	20.9	>99	-
9	I	TEA	4	−20	8.54	30 000	1.97	18 200	256	18.0	>99	-
10	I	TEA	6	−20	6.02	21 300	1.89	12 200	255	16.6	>99	-
11	I	TEA	8	−20	5.45	15 800	1.81	9800	251	10.4	>99	-
12	I	TEA	25	−20	1.95	7900	1.78	5600	248	9.9	>99	-
13	II	TEA	2	20	3.89	9800	1.65	6100	244	7.8	80.0	20.0
14	II	TEA	8	20	1.53	4400	1.53	2500	241	4.7	84.2	15.8
15	II	TEA	8	0	0.89	8600	1.65	5100	244	7.8	92.3	7.7
16	II	TMA	8	20	0.53	5100	1.81	3000	235	4.2	79.2	20.8

[a]Catalyst **I**: $Me_2C(Cp)(Flu)ZrCl_2$; Catalyst **II**: $Ph_2Si(Cp)(Flu)ZrCl_2$. [b]TEA = triethylaluminum. [c]Acticity = kg sPATMS·mol^{-1}Zr·h^{-1} [d]M_n (number-average molecular weight), M_w (weight-average molecular weight), and PDI (polydispersity, M_w/M_n) were determined by high temperature GPC (solvent, tetratydrofuran ; temperature 40 °C.). [e]M_n calculated by ^{1}H NMR. [f]T_m, (melting temperature), -ΔH(enthalpy of melting temperature) was determined by DSC. [g]The end group ratios were determined by 500 MHz ^{1}H NMR analyses (solvent, $CDCl_3$; temperature 60 °C). [h]Polymerization conditions: 30 mL of toluene; 31.5 mmol of ATMS (allyltrimethylsilane); 12.5 μmol of catalyst; 25.0 mmol of MAO; reaction time = 24 h.

generation of macroinitiator. Then, the reaction vessel was charged with 1.60 g of MMA (16.0 mmol) and allowed to undergo the chain-extension reaction at 95 °C for 24 h. The resulting solution was collected by filtration to remove insoluble copper metal complexes. The resulting polymer solution was concentrated to 15 mL via the removal of volatiles under vacuum. The resulting solution was charged with excess methanol (ca. 20 mL), which led to the deposition of the reaction product as an off-white precipitate. The resulting precipitate was isolated by filtration and allowed to undergo Soxhlet extraction with boiling cyclohexane to remove residual sPATMS. The resulting sPATMS-*b*-PMMA was dried under vacuum for 24 h to provide 1.02 g of sPATMS-*b*-PMMA [M_n = 45500, M_w/M_n = 1.29 as determined by GPC (in THF at 40 °C).

Characterization of Polymers. The molecular weight and molecular weight distribution (MWD) of synthesized polymers were determined by using GPC (Waters 2410-CALAC/GPC) with a refractive index (RI) detector and a set of U-Styragel HT columns with 10^6, 10^5, 10^4, and 10^3 Å pore sizes in series. The measurements were taken at 40 °C using THF as solvent. Polystyrene (PS) samples with narrow MWDs were used as the standards for calibration. The standards were in the range of absolute molecular weight from 980 to 2,110 000 g/mol; the *R* square of the ideal calibrated line was limited up to 0.999.

All ^{1}H and ^{13}C NMR spectra were recorded on a Bruker AV-500 NMR spectrometer. The sPATMS-based samples were dissolved in $CDCl_3$ or benzene-d_6. The recorded temperature was 60 °C.

Preparation of Bulk Samples. Bulk samples of sPATMS-*b*-PMMA BCPs were prepared by solution casting from a nonselective solvent, dichloromethane (CH_2Cl_2), at a concentration of 10 wt % sPATMS-*b*-PMMA at room temperature. After completely dissolving the polymers, the solution was filtrated through a filter with 0.45 μm pathways to remove impurities. The solution was then transferred to a vial and sealed well by aluminum foil with punch holes for the slow evaporation of the solvent. After drying, the bulk samples were further dried in a vacuum oven to remove residual solvent.

Characterization of Nanostructures. Bright-field transmission electron microscopy (TEM) images were obtained by using a JEOL JEM-2100 LaB_6 transmission electron microscope at an accelerating voltage of 200 kV. The bulk samples were sectioned at room temperature by using a Leica ultramicrotome. The microsections were collected on copper grids (100 mesh) with polyvinyl formal as a supporting membrane and covered by a thin film of carbon to protect the unstained samples from the electron damages such as shrinkage and degradation. For these silyl-containing BCPs, no staining procedure was required to enhance the mass−thickness contrast because the atomic number of silicon is obviously higher than that of carbon and oxygen. Accordingly, the sPATMS domains exhibited dark regions while the PMMA blocks appeared bright areas under TEM observations due to the intrinsic mass−thickness contrast. Small-angle X-ray scattering (SAXS) experiments were conducted at the synchrotron X-ray beamline 23A1 at the National Synchrotron Radiation Research Center (NSRRC) in Hsinchu, Taiwan.

RESULTS AND DISSCUSSION

Synthesis of Hydroxyl-Capped sPATMS by Selective Chain Transfer to Alkylauminum.[25] The synthesis of OH-capped sPATMS via the selective chain transfer to alkylaluminum were investigated by syndiospecific polymerization of allyltrimethylsilane (ATMS) conducted in the presence of two *ansa*-metallocene catalysts [$(Me)_2C(Cp)(Flu)ZrCl_2$ (**I**) and $(Me)_2Si(Cp)(Flu)ZrCl_2$ (**II**)] using TEA as the chain transfer agent. The selective chain transfer reaction to TEA led to the generation of alkylaluminum-capped sPATMS as the preliminary product. After polymerization, the polymer solution was in situ treated with O_2/H_2O_2[13a,b,26] for converting the aluminum end group into a stable hydroxyl terminal group; this led to the generation of OH-capped sPATMS as the final reaction product. The resulting polymer solution was then charged with excess methanol, leading to the deposition of the ATMS-based polymer as a white precipitate, which can be isolated after filtration. The ^{1}H and ^{13}C NMR spectra of the ATMS-based polymers synthesized under these conditions were evaluated to determine the chain end structures. The results of the polymerization studies are summarized in Table 1.

There are four possible chain releasing pathways, which lead to the generation of sPATMSs with characteristic hydroxy,

dx.doi.org/10.1021/ma300034f | Macromolecules 2012, 45, 2720−2730

Scheme 1. Probable Polymer Chain End in Syndiotactic Poly(allyltrimethylsilane) Synthesis by Metallocene

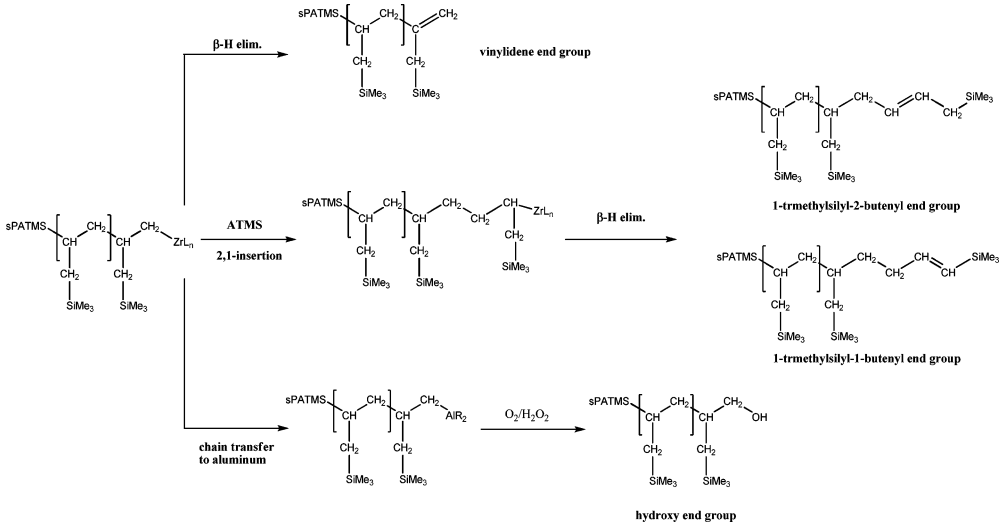

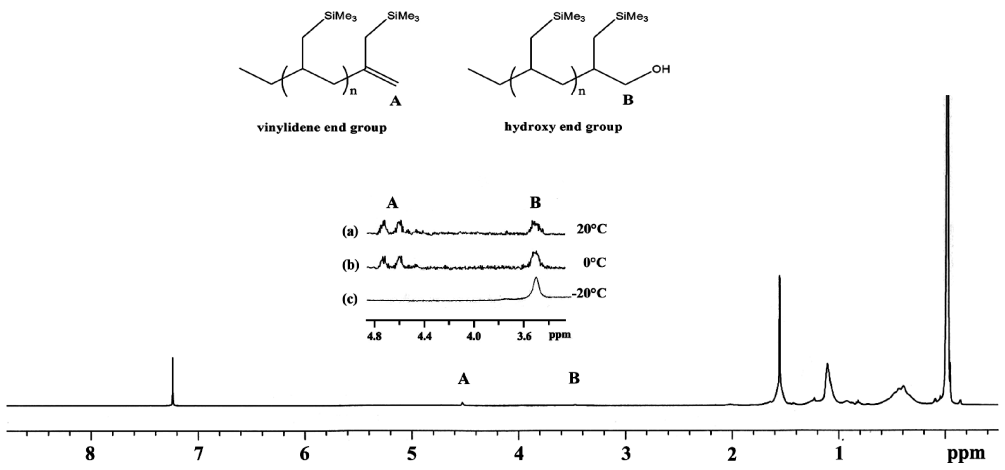

Figure 1. Expanded ^{1}H NMR (500 MHz) region of various sPATMS samples (a) M_n = 4600 g/mol, M_w/M_n = 1.54 (entry 4 of Table 1), (b) M_n = 14800 g/mol, M_w/M_n = 1.70 (entry 6 of Table 1), (c) M_n = 7900 g/mol, M_w/M_n = 1.78 (entry 12 of Table 1) (solvent, $CDCl_3$; temperature 60 °C).

vinylidene, 1-trimethylsilyl-1-butenyl, and 1-trimethylsilyl-2-butenyl end groups, respectively, as illustrated in Scheme 1. As shown in Figure 1 (entries 4, 6, and 12 of Table 1), sPATMSs with two different chain end structures, namely hydroxyl and vinylidene end groups, can be generated under these reaction conditions. The hydroxyl end group was produced from the 1,2- insertion of a terminal ATMS unit, which underwent chain transfer to aluminum to give aluminum-capped sPATMS as the preliminary reaction product; subsequently, the in situ oxidation of the resulting aluminum-capped sPATMS by the method described in the experiment section led to the generation of OH-capped sPATMS. The vinylidene chain end was generated from the 1,2-insertion of a terminal ATMS unit, which, in contrast, underwent β-hydride elimination chain transfer. It is noted that we were unable to detect the formation of 1-trimethylsilyl-1-butenyl-capped sPATMS [$(CH_3)_3Si-CH{=}CH-CH_2-CH_2-$sPATMS] and 1-trimethylsilyl-2-butenyl-capped sPATMS [$(CH_3)_3Si-CH2-CH{=}CH-CH_2-$sPATMS] generated from the 2,1-insertion of a terminal ATMS unit, which underwent subsequent β-hydride elimination transfer by abstracting methylene hydrides at the α- and γ-positions, respectively, from the terminal trimethylsilyl group. The generations of OH-capped and vinylidene-capped sPATMSs without 1-trimethylsilyl-1-butenyl-capped and 1-trimethylsilyl-2-butenyl-capped sPATMSs reveals that the insertion of ATMS follows the predominant 1,2-insertion patterns and that OH-capped sPATMS and vinylidene-capped sPATMS were generated from the 1,2-inserted terminal ATMS unit, which underwent a subsequent chain transfer reaction to TEA and the β-hydride elimination chain transfer reaction, respectively.

Although the syndiospecific ATMS polymerization conducted in the presence of these *ansa*-metallocene catalysts provides perfect regioselectivity (predominant 1,2-insertion) control, the formation of sPATMSs containing two different terminal groups (hydroxyl and vinylidene end groups; see entries 1−7 of Table 1) indicates that these catalyst systems fail to facilitate chain-end structural control through regulating chain transfer mechanisms especially when polymerization was conducted at a high polymerization temperature. The results listed in Table 1 reveal that the formation of OH-capped sPATMS via the selective chain transfer to alkylaluminums depends on the structures and concentration of chain transfer agents. As shown in entry 1−5 of Table 1, β-hydride elimination transfer (producing vinylidene-capped sPATMS) was the predominant chain releasing pathway

dx.doi.org/10.1021/ma300034f | *Macromolecules* 2012, 45, 2720−2730

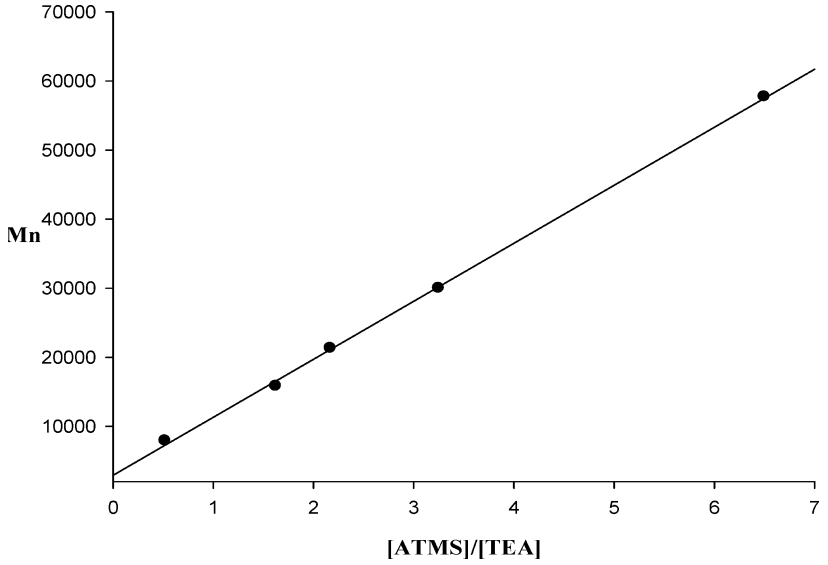

Figure 2. Plot of number-average molecular weight (M_n) of OH-capped sPATMS vs the mole ratios of [ATMS]/[TEA] (entries 8−12 of Table 1).

when polymerization was conducted at high temperature (≥20 °C). In contrast, syndiospecific ATMS polymerization conducted at low temperature (≤20 °C) shifted the chain releasing pathway from β-hydride elimination transfer to mainly the chain transfer to alkylaluminums. A comparison of entries 6−7 and 14−16 of Table 1 shows that replacing TMA with TEA led to the production of an increased amount of OH-capped sPATMS and that the amount of OH-capped sPATMS can be enhanced by increasing the concentration of trialkylaluminum in the feed. Although increasing the concentration of TEA increases the amount of OH-capped sPATMS, OH-capped sPATMS cannot be prepared as a single reaction product since these reaction conditions also generate vinylidene-capped sPATMS, which is generated through β-hydride elimination transfer, as the minor reaction product.

In order to provide pure OH-capped sPATMS for use as the end-functionalized prepolymer in the synthesis of stereoregular BCPs, syndiospecific polymerizations of ATMS at a lower temperature (−20 °C)[13b,27] were conducted to suppress the β-hydride elimination transfer for the formation of vinylidene-capped sPATMS. Entries 8−12 of Table 1 show that OH-capped sPATMS can be selectively produced as the only detectable product (by NMR analyses) at low temperature. Figure 2 shows the plot of polymer molecular weight versus [ATMS]/[TEA] by conducting the allyltrimethylsilane polymerization at −20 °C using $(Me)_2C(Cp)(Flu)ZrCl_2$ (**I**) as the catalyst and TEA as the chain transfer agent (entries 8−12). The nearly linear relationship between the molecular weight of sPATMSs and [ATMS]/[TEA] ratio indicates that chain transfer to TEA (rate constant = k_{tr}) competes with the allyltrimethylsilane chain propagation reaction. Since the degree of polymerization (X_n) follows the equation $X_n = k_p[ATMS]/k_{tr}[TEA]$, the plot in Figure 2 can be used to calculate the chain transfer constant (k_{tr}/k_p = 1/35.5) for the generation of OH-capped sPATMS by predominant chain transfer to TEA. Nevertheless, OH-capped sPATMS can be selectively generated by selective chain transfer to TEA during syndiospecific polymerization of allyltrimethylsilane conducted in the presence of syndiospecific metallocene catalysts.

End Group Analyses of Hydroxyl-Capped sPATMS. End group analyses provide detailed structural information for the resultant ATMS polymers and give direct evidence of the successful preparation of pure OH-capped sPATMS. Figure 1c shows the ^{1}H NMR spectrum (with an inset showing the expanded region and chemical shift assignments) of the OH-capped sPATMS (M_n = 7900 g/mol, M_w/M_n = 1.78; entry 12 of Table 1) isolated after the O_2/H_2O_2 treatment. As shown in the ^{1}H NMR spectrum, in addition to the four major upfield resonances (δ = 0.31, 0.42, 1.13, 1.65) corresponding to the $-CH[CH_2Si(C\mathbf{H}_3)_3]-CH_2-$, $-CH[C\mathbf{H}_2Si(CH_3)_3]-CH_2-$, $-CH[CH_2Si(CH_3)_3]-C\mathbf{H}_2-$ and $-C\mathbf{H}[CH_2Si(CH_3)_3]-CH_2-$ proton resonances of the sPATMS backbone, respectively, there is a weak downfield resonance at 3.47 ppm, which corresponds to the chain end $-CH[CH_2Si(CH_3)_3]-C\boldsymbol{H}_2-OH$ proton resonance. The detailed chemical assignments are based on the structural information on [^{13}C (DEPT 135); Figure 3] and [two-dimensional ^{1}H−^{13}C HMQC; Supporting Information] NMR spectra. These NMR spectra clearly reveal that OH-capped sPATMS prepared by selective chain transfer to TEA has a single hydroxyl terminal group, making it suitable for use as a stereoregular end-functionalized prepolymer in the construction of stereoregular BCPs. Two aliphatic chain ends, 2-(trimethylsilylmethyl)-butyl [$CH_3CH_2CH(CH_2SiMe_3)CH_2-$] (approximately 88% based on integration) and 2-(trimethylsilylmethyl)propyl [$CH_3CH(CH_2SiMe_3)CH_2-$] (approximately 12% based on integration), generated in the chain initiation steps, can be identified by ^{13}C NMR analyses (Figure 3). The [$CH_3CH_2CH(CH_2SiMe_3)CH_2-$] end group was generated in the chain initiation step by the primary insertion of allyltrimethylsilane to [Zr−Et], formed in the chain releasing step by selective chain transfer to TEA. The [$CH_3CH(CH_2SiMe_3)CH_2-$] end group was generated by the primary insertion of allyltrimethylsilane to [Zr−Me], which was formed in the chain releasing step by chain transfer to MAO.

Synthesis of Silyl-Containing Stereoregular BCPs. As demonstrated by the chain end analysis, OH-capped sPATMS prepared by the selective chain transfer route contains a single hydroxyl end group, making it suitable for use as the end-functionalized macroinitiator for the synthesis of stereoregular BCPs. Unfortunately, the OH-capped sPATMS macroinitiator prepared via the metallocene-catalyst-mediated selective chain transfer route has a broad range of molecular weight distribution, and hence is not suitable for use directly in the post block

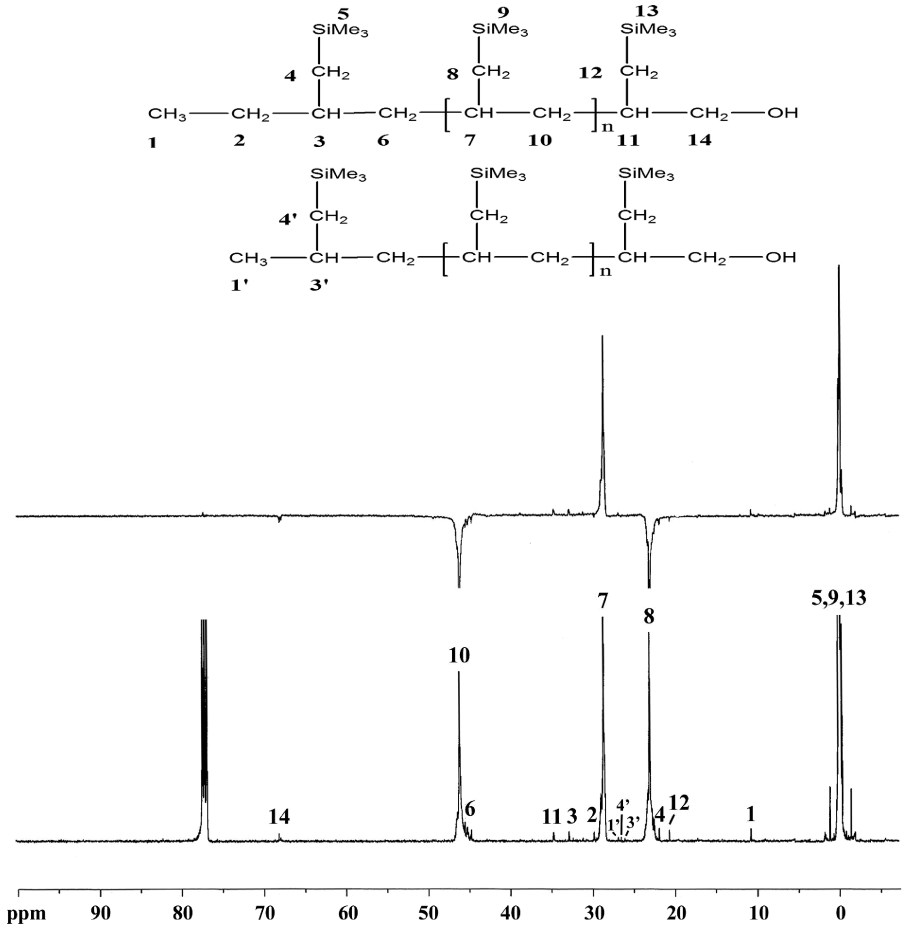

Figure 3. ^{13}C (DEPT-135) NMR (125 MHz) spectra of OH-capped sPATMS (M_n = 15800 g/mol, M_w/M_n = 1.81; entry 11 of Table 1) (solvent, $CDCl_3$; temperature 60 °C).

polymerization reaction for the preparation of structurally well-defined stereoregular BCPs. Although BCPs with relatively high polydispersity are capable of self-organizing into ordered morphologies, the broad distribution in chain length shifts the phase boundaries (relative to those of the corresponding monodisperse BCPs) and modifies the microdomain size.[28] Narrow-MWD samples of OH-capped sPATMSs are preferred for use as the end-functionalized stereoregular prepolymer for the preparation of structurally well-defined sillyl-containing stereoregular BCPs.[13b,c] Narrow-MWD samples of end-functionalized stereoregular polymers can be obtained by the fractionation of the broad-MWD product through extraction processes, as demonstrated by prior reports.[13,29] Thus, fractionation of the broad-MWD product (M_n = 15800, M_w/M_n = 1.81) by Soxhlet extractions in MEK/THF (3:1) using methods described in the Experimental Section giving a narrow-MWD sample of OH-capped sPATMS (M_n = 13100, M_w/M_n = 1.40). The hydroxyl terminal group of OH-capped sPATMS was allowed to convert into the α-bromoester end group by the reaction between the OH-capped sPATMS and α-bromoisobutyryl bromide to provide α-bromoester-terminated sPATMS with high yield. The comparison of the ^1H NMR spectra of OH-capped sPATMS (M_n = 13100 g/mol, M_w/M_n = 1.40) with that of α-bromoester-capped sPATMS (M_n = 13200 g/mol, M_w/M_n =1.40) is shown in Figure 4. The resulting α-bromoester-terminated sPATMS was in situ treated with CuBr and was chain-extended with MMA by the controlled/living radical polymerization of MMA to give sPATMS-*b*-PMMA (M_n = 42600 g/mol, M_w/M_n = 1.30)

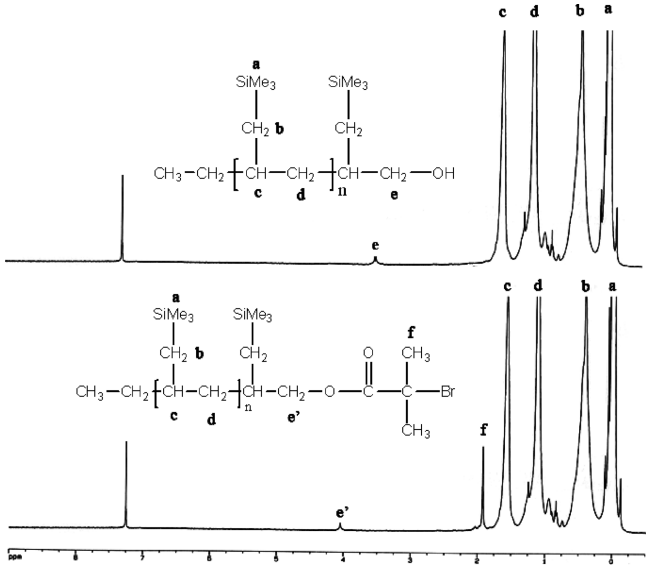

Figure 4. ^1H NMR spectra (500 MHz) of (a) OH-capped sPATMS (M_n = 13300 g/mol, M_w/M_n = 1.40), (b) Br-capped sPATMS (M_n = 13500 g/mol, M_w/M_n =1.40) (solvent, $CDCl_3$; temperature 60 °C).

as a structurally well-defined silyl-containing stereoregular diblock copolymer with a good MMA conversion ratio and high BCP yield. The detailed synthetic routes for the preparation of sPATMS-*b*-PMMA are illustrated in Scheme 2. The comparison of the GPC

dx.doi.org/10.1021/ma300034f | *Macromolecules* 2012, 45, 2720−2730

Scheme 2. Synthetic Routes for Preparations of End-Functionalized sPATMS and sPATMS-Based Stereoregular Block Copolymers

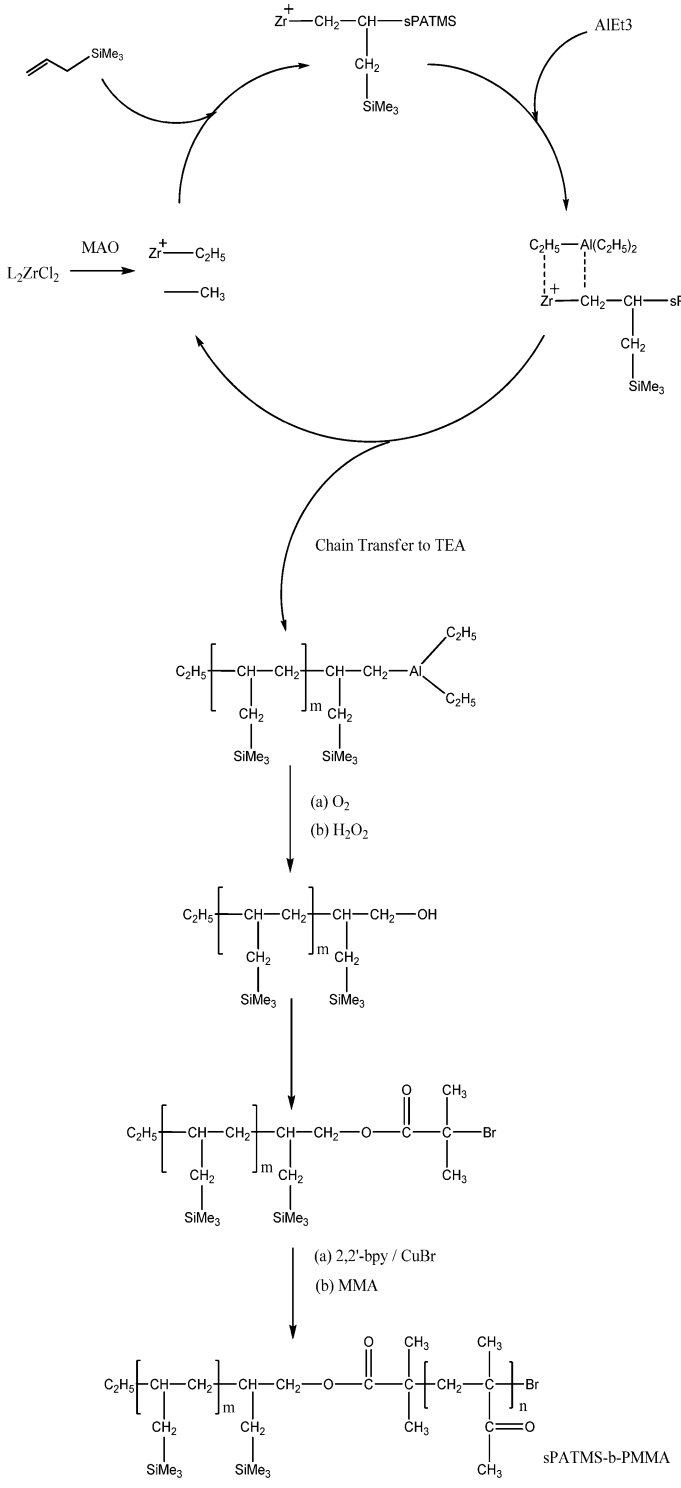

elution curves of OH-capped sPATMS with that of sPATMS-*b*-PMMA (M_n = 42600 g/mol, M_w/M_n = 1.30) is shown in Figure 5. Figures 6 show the ^{1}H NMR spectrum (with insets showing chemical shift assignments) of sPATMS-*b*-PMMA. [The ^{13}C (DEPT 135) NMR spectra can be found in Supporting Information]. The proposed synthetic route is further illustrated by the preparation of a second sPATMS-*b*-PMMA sample (M_n = 29900 g/mol, M_w/M_n = 1.24; GPC and ^{1}H NMR spectrum of this sample can be found in the Supporting Information) from the same narrow-MWD end-functionalized α-bromoester-capped sPATMS (M_n = 13500 g/mol, M_w/M_n = 1.40).

Self-Assembled Nanostructures of Stereoregular BCPs. Owing to the stereoregularity of the sPATMS block, the synthesized sPATMS-*b*-PMMA samples show semicrystalline behavior. The thermal behavior of the sPATMS-*b*-PMMA was first examined by DSC. The DSC thermograms were recorded during the second heating cycle from 0 to 270 °C with a heating rate of 10 °C/min after fast cooling by 150 °C/min

dx.doi.org/10.1021/ma300034f | *Macromolecules* 2012, 45, 2720−2730

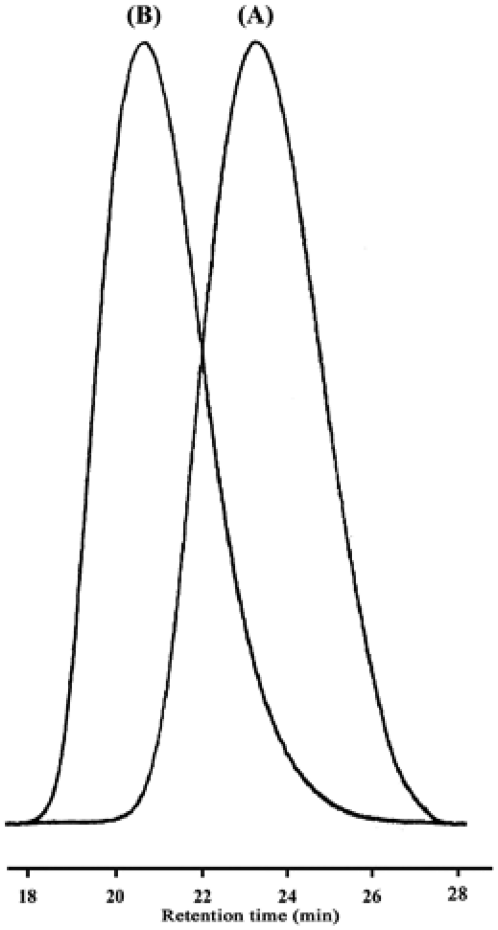

Figure 5. The GPC curves comparison between (A) OH-capped sPATMS (M_n = 13500 g/mol, M_w/M_n = 1.40), (B) sPATMS-*b*-PMMA (M_n = 45500 g/mol, M_w/M_n = 1.29) (in THF, at 40 °C).

from the melt sate of samples at 270 °C. From DSC profiles of the second heating process (Figure 7), the sPATMS-*b*-PMMA with various volume fractions of sPATMS exhibit different thermal properties. For sPATMS13-PMMA32 with a lower volume fraction of PLLA (i.e., f^{v}_{sPATMS} = 0.35), the glass transition temperatures (T_g) of sPATMS and PMMA blocks were determined as approximately 36 and 117 °C, respectively (Figure 7a). The absence of a sPATMS crystallization temperature and melting point in the high temperature region is attributed to the confinement effect for sPATMA chains restricted in the PMMA matrix. For comparison, sPATMS13-PMMA17 with a higher volume fraction of sPATMS (i.e., f^{v}_{sPATMS} = 0.51) gives glass transition temperatures of sPATMS and PMMA blocks at approximately 36 and 105 °C, respectively (Figure 7b). The slightly lower $T_{g,PMMA}$ of sPATMS13-PMMA17 than that of sPATMS13-PMMA32 is attributed to the molecular weight effect. In contrast to the amorphous behavior of sPATMS in sPATMS13-PMMA32, a small endothermic peak at 232 °C for the sPATMS melting point (T_m) can be observed in the high temperature region,[17] further confirming the confined effect on the crystallization of sPATMS chains in sPATMS13-PMMA17.

To achieve the formation of well-ordered nanostructures from the self-assembly of sPATMS-*b*-PMMA BCPs in the bulk state, the bulk samples of sPATMS-*b*-PMMA were first heated to the maximum annealing temperature, T_{max} = 270 °C, for 3 min to eliminate the sPATMS crystalline residues resulting from sample preparation. Subsequently, the thermally treated bulk samples could be obtained after rapidly cooling at a rate of 150 °C/min from the melt state at 270 °C. For sPATMS13-PMMA32 (f^{v}_{sPATMS} = 0.35), hexagonally packed cylindrical nanostuctures were observed in TEM images (Figure 8a). Owing to the higher atomic number of silicon than that of carbon and oxygen, the dark cylinders can be referred to the sPATMS microdomains and dispersed in the bright PMMA matrix under TEM observation. The self-assembled morphology can be further identified

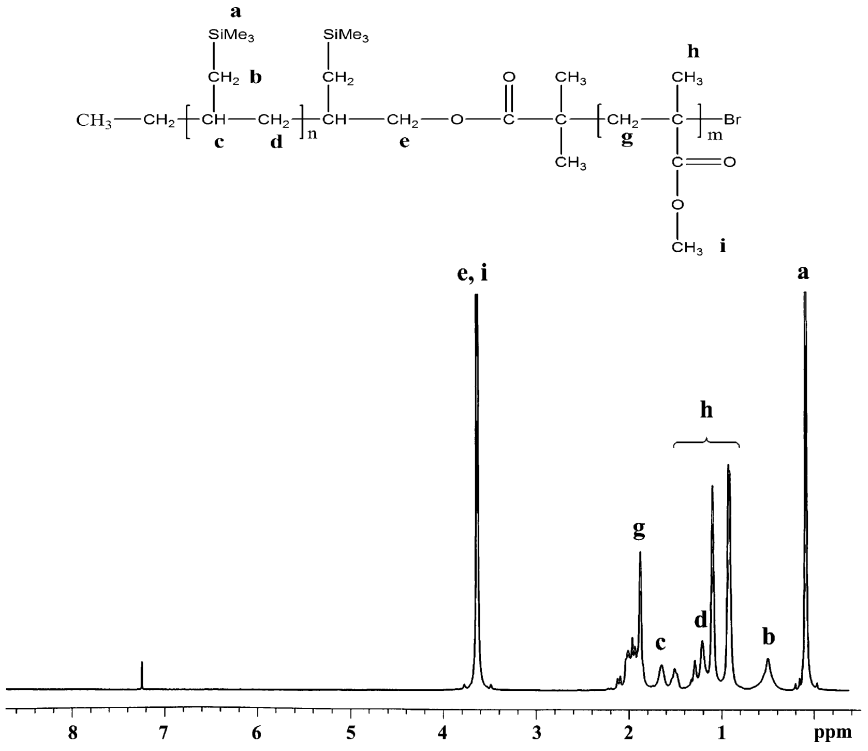

Figure 6. ^{1}H (500 Hz) NMR spectrum of sPATMS-*b*-PMMA (M_n = 45500 g/mol, M_w/M_n = 1.29, f_{sPATMS} = 0.35) (solvent, $CDCl_3$; temperature 60 °C).

dx.doi.org/10.1021/ma300034f | *Macromolecules* 2012, 45, 2720−2730

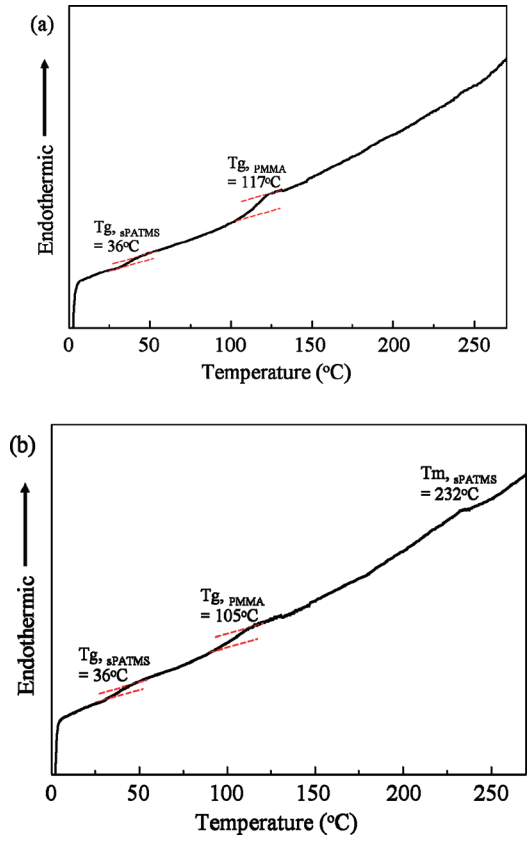

Figure 7. DSC thermograms of sPATMS–PMMA with sPATMS volume fraction of (a) 0.35 and (b) 0.51, respectively. The heating rate is 10 °C/min.

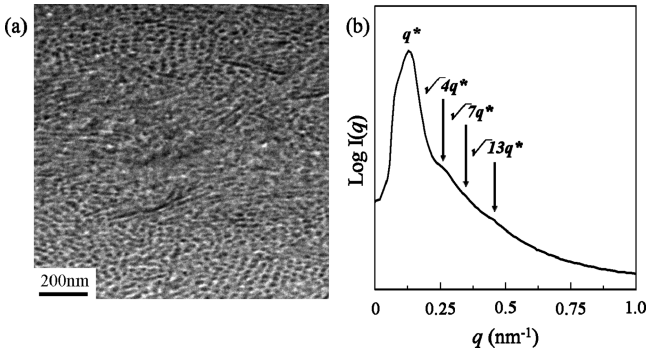

Figure 8. (a) TEM micrographs of sPATMS–PMMA (f^{v}_{sPATMS} = 0.35) block copolymer with hexagonally packed cylinder nanostructure. The microdomains of sPATMS appear dark while the PMMA microdomain displays bright. (b) Corresponding one-dimensional SAXS profile.

by SAXS experiments. Corresponding one-dimensional SAXS profile (Figure 8b) shows well-ordered reflections with peak positions at the q ratios of $1:\sqrt{4}:\sqrt{7}:\sqrt{13}$, indicating a well-ordered cylindrical phase with hexagonal packing. Using the primary peak, the d-spacing of the (100) plane was determined as 49.3 nm and the interspacing of each cylinder was then calculated as 56.9 nm. These results suggest that the crystallization temperature of sPATMS is below the order–disorder transition temperature (T_{ODT}) and the self-assembled nanostructure driven from the incompatibility of the sPATMS and PMMA blocks can be successfully developed. In contrast,

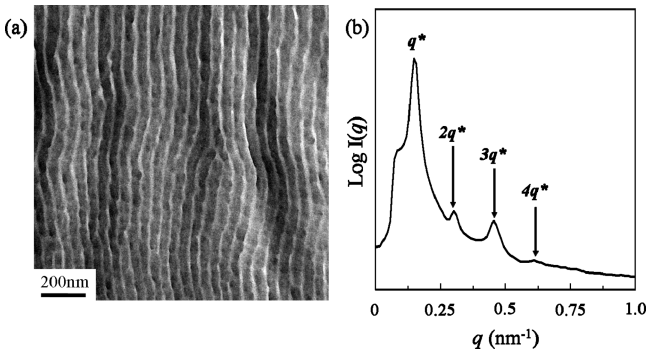

Figure 9. (a) TEM micrographs of sPATMS–PLLA (f^{v}_{PLLA} = 0.51) block copolymer with lamellar nanostructure. The microdomains of sPATMS appear dark while the PMMA microdomain displays bright. (c) Corresponding one-dimensional SAXS profile.

Figure 9a shows the lamellar nanostructure of sPATMS13-PMMA17 (f^{v}_{sPATMS} = 0.51) resulting from the self-assembly in the melt state. For SAXS experiments, the self-assembled morphology of the sPATMS-*b*-PMMA is identified as a lamellar phase according to the reflection peaks at the q ratios of 1: 2: 3: 4 (Figure 9b). The d-spacing of the (100) plane was determined as 42.9 nm from the primary peak of the reflections.

CONCLUSIONS

The preparations of structurally well-defined silyl-containing stereoregular BCPs composed of syndiotactic polytrimethylallylsilane (sPATMS) and poly(methyl methacrylate) (PMMA) through the controlled living atom transfer radical polymerization (ATRP) of methyl methacrylate using α-bromoester end-capped sPATMS for the in situ generation of CuBr-capped macroinitiator was presented. The α-bromoester end-capped sPATMS was generated via the esterification of hydroxyl-capped sPATMS with α-bromoisobutyl bromide. Hydroxyl-capped sPATMS was produced by inducing the selective chain transfer reaction to trialkylaluminum during the syndiospecific polymerization of allytrimethylsilane. This work is the first example to prepare the sily functional-moieties containing stereoregular diblock copolymers, which have a well-defined chemical architecture with uniform molecular length, and which can self-organize into the consistent morphologies, as revealed by TEM and SAXS examinations.

ASSOCIATED CONTENT

Supporting Information

^{13}C (DEPT-135) and two-dimensional ^{1}H and ^{13}C HMQC NMR spectra of α-bromoester-capped sPATMS and ^{1}H NMR spectrum and GPC curves of sPATMS-*b*-PMMA. This material is available free of charge via the Internet at http://pubs.acs.org.

AUTHOR INFORMATION

Corresponding Author

*(J.-C.T.) Telephone: 886-5-2720411 ext 33460. Fax: 886-5-2721206. E-mail: chmjct@ccu.edu.tw. (R.-M.H.) Telephone: 886-3-5738349. Fax 886-3-5715408. E-mail: rmho@mx.nthu.edu.tw.

Notes

The authors declare no competing financial interest.

■ ACKNOWLEDGMENTS

Authors would like to thank the National Science Council of Taiwan for the financial support for this research under contracts NSC-99-2221-E-194-003 and NSC-99-2120M-E-007-013.

■ REFERENCES

(1) (a) Lehn, J.-M. *Science* **1985**, *227*, 849−856. (b) Whitesides, G. M.; Grzybowski, B. *Science* **2002**, *295*, 2418−2421.

(2) (a) Lehn, J.-M. *Proc. Natl. Acad. Sci. U.S.A.* **2002**, *99*, 4763−4768. (b) Whitesides, G. M.; Boncheva, M. *Proc. Natl. Acad. Sci. U.S.A.* **2002**, *99*, 4769−4774.

(3) (a) Thomas, E. L.; Anderson, D. M.; Henkee, C. S.; Hoffman, D. *Nature* **1988**, *344*, 598−601. (b) Muthukumar, M.; Ober, C. K.; Thomas, E. L. *Science* **2002**, *277*, 1225−1232.

(4) (a) Bates, F. S.; Fredrickson, G. H. *Annu. Rev. Phys. Chem.* **1990**, *41*, 525−557. (b) Matsen, M. W.; Schick, M. *Phys. Rev. Lett.* **1994**, *72*, 2660−2663. (c) Matsen, M. W.; Bates, F. S. *Macromolecules* **1996**, *29*, 1091−1098. (d) Matsen, M. W.; Bates, F. S. *Macromolecules* **1996**, *29*, 7641−7644. (e) Bates, F. S.; Fredrickson, G. H. *Phys. Today* **1999**, *52*, 32−38.

(5) (a) Cohen, R. E.; Cheng, P.-L.; Douzinas, K.; Kofinas, P.; Berney, C. V. *Macromolecules* **1990**, *23*, 324−327. (b) Loo, Y. -L.; Register, R. A.; Ryan, A. J. *Macromolecules* **2002**, *35*, 2365−2374. (c) Ho, R.-M.; Lin, F.-H.; Tsai, C.-C.; Lin, C.-C.; Ko, B.-T.; Hsiao, B. S.; Sics, I. *Macromolecules* **2004**, *37*, 5985−5994. (d) Chen, C.-K.; Lin, S.-C.; Chiang, Y.-W.; Ho, R.-M.; Latz, B. *Macromolecules* **2010**, *43*, 7752−7758.

(6) (a) Chiang, Y.-W.; Ho, R.-M.; Ko, B.-T.; Lin, C.-C. *Angew. Chem., Int. Ed. Engl.* **2005**, *44*, 7969−7972. (b) Chiang, Y.-W.; Ho, R.-M.; Thomas, E. L.; Burger, C.; Hsiao, B. S. *Adv. Funct. Mater.* **2009**, *19*, 448−459.

(7) (a) Lin, Z.; Kim, D. H.; Wu, X.; Boosahda, L.; Stone, D.; LaRose, L.; Russell, T. P. *Adv. Mater.* **2002**, *14*, 1373−1376. (b) Qiao, Y.; Wang, D.; Buriak, J. M. *Nano Lett.* **2007**, *7*, 464−469. (c) Thurn-Albrecht, T.; Steiner, R.; DeRouchey, J.; Stafford, C. M.; Huang, E.; Bal, M.; Tuominen, M.; Hawker, C. J.; Russell, T. P. *Adv. Mater.* **2000**, *12*, 787−791. (d) Zalusky, A. S.; Olayo-Valles, R.; Taylor, C. J.; Hillmyer, M. A. *J. Am. Chem. Soc.* **2001**, *123*, 1519−1520. (e) Lo, K.-H.; Tseng, W.-H.; Ho, R.-M. *Macromolecules* **2007**, *40*, 2621−2624. (f) Lo, K.-H.; Chen, M.-C.; Ho, R.-M.; Sung, H.-W. *ACS Nano* **2009**, *3*, 2660−2666.

(8) (a) Tseng, W.-H.; Chen, C.-K.; Chiang, Y.-W.; Ho, R.-M.; Akasaka, S.; Hasegawa, H. *J. Am. Chem. Soc.* **2009**, *131*, 1356−1357. (b) Hsueh, H.-Y.; Chen, H.-Y.; She, M.-S.; Chen, C.-K.; Ho, R.-M.; Gwo, S.; Hasegawa, H.; Thomas, E. L. *Nano Lett.* **2010**, *10*, 4994−5000.

(9) (a) Arkles, B. *Chem. Tech.* **1983**, *13*, 542−555. (b) Noll, W. *Chemistry and Technology of Silicones*: Academic Press: New York, 1968. (c) Tomanek, A. *Silicones and Industry*: Hanser (Wacker Chemie): Munich, Germany, 1991. (d) Beevers, M. S. *Dielectric Properties of Siloxanes, In Siloxane Polymers*, Clarson, S. J.; Semlyen, J. A.; Eds.; Prentice Hall: Englewood Cliffs, NJ, 1993. (e) Baker, E. B.; Barry, A. J.; Hunter, M. *J. Ind. Eng. Chem.* **1946**, *38*, 1117−1120. (f) Warrick, E. L.; Hunter, M. J.; Barry, A. *J. Ind. Eng. Chem.* **1952**, *44*, 2196−2202. (g) Young, O. B.; Dickerman, C. E. *Ind. Eng. Chem.* **1954**, *46*, 364−365. (h) ÅKerlöf, G. *J. Am. Chem. Soc.* **1932**, *54*, 4125−4139. (i) Chang, P.-S.; Buese, M. A. *J. Am. Chem. Soc.* **1993**, *115*, 11475−11484. (j) Thomas, D. R. *Crosslinking of Silicones, In Siloxane Polymers*; Clarson, S. J., Semlyen, J. A., Eds.; Prentice Hall: Englewood Cliffs, NJ, 1993. (k) Plate, N. A.; Durgarjan, S. G.; Khotimskii, V. S.; Teplyakov, V. V.; Yampolskii, Y. P. *J. Membrane Sci.* **1990**, *52*, 289−304. (l) Wang, C.; Wang, J.; Park, C. B.; Kim, Y.-W. *J. Mater. Sci.* **2004**, *39*, 4913−4915. (m) Hewitt, D. G.; Jing, L. *J. Polym. Sci., Part A: Polym. Chem.* **1998**, *36*, 1093−1106.

(10) Bita, I.; Yang, J. K. W.; Jung, Y. S.; Ross, C. A.; Thomas, E. L.; Berggren, K. K. *Science* **2008**, *321*, 939−943. (b) Lammertink, R. G. H.; Hempenius, M. A.; van den Enk, J. E.; Chan, V. Z.-H.; Thomas, E. L.; Vancso, G. J. *Adv. Mater.* **2000**, *12*, 98−103. (c) Park, C.; Yoon, J.; Thomas, E. L. *Polymer* **2003**, *44*, 6725−6760. (d) Guo, L. J. *Adv. Mater.* **2007**, *19*, 495−513. (e) Chemg, J. Y.; Ross, C. A.; Chan, V. Z. H.; Thomas, E. L.; Lammertink, R. G. H.; Vancso, G. J. *Adv. Mater.* **2001**, *13*, 1174−1178. (f) Choi, P.; Fu, P.-F.; Guo, L. J. *Adv. Funct. Mater.* **2007**, *17*, 65−70. (g) Chao, C.-C.; Ho, R.-M.; Georgopanos, P.; Avgeropoulos, A.; Thomas, E. L. *Soft Matter* **2010**, *6*, 3582−3587. (h) Chao, C.-C.; Ho, R.-M.; Georgopanos, P.; Avgeropoulos, A.; Thomas, E. L. *ACS Nano* **2010**, *4*, 2088−2094.

(11) (a) Gilroy, J. B.; Gädt, T.; Whittell, G. R.; Chabanne, L.; Mitchels, J. M.; Richardson, R. M.; Winnik, M. A.; Manners, I. *Nat. Chem.* **2010**, *2*, 566−570. (b) Massey, J. A.; Temple, K.; Cao, L.; Rharbi, Y.; Raez, J.; Winnik, M. A.; Manners, I. *J. Am. Chem. Soc.* **2000**, *122*, 11577−11584. (c) Ni, Y.; Rulkens, R.; Manners, I. *J. Am. Chem. Soc.* **1996**, *118*, 4102−4114. (d) Elio, J. C.; Rider, D. A.; Wang, J. Y.; Russell, T. P.; Manners, I. *Macromolecules* **2008**, *41*, 9474−9479. (e) Soto, A. P.; Manners, I. *Macromolecules* **2009**, *42*, 40−42. (f) He, F.; Gädt, T.; Jones, M.; Scholes, G. D.; Manners, I.; Winnik, M. A. *Macromolecules* **2009**, *42*, 7953−7960. (g) Chen, H.; Wu, X.; Duan, H.; Wang, Y. A.; Wang, L.; Zhang, M.; Mao, H. *ACS Appl. Mater. Interfaces* **2009**, *1*, 2134−2140. (h) Raez, J.; Manners, I.; Winnik, M. A. *J. Am. Chem. Soc.* **2002**, *124*, 10381−10395. (i) Wang, X. S.; Winnik, M. A.; Manner, I. *Macromolecules* **2002**, *35*, 9146−9150. (j) Cao, L.; Manners, I.; Winnik, M. A. *Macromolecules* **2002**, *35*, 8258−8260. (k) Massey, J. A.; Power, K. N.; Manners, I.; Winnik, M. A. *Adv. Mater.* **1998**, *10*, 1559−1562.

(12) (a) Hani, R.; Lenz, R. W. *Silicon-based Polymer science: a comprehensive resource*; Zeigler, J. M., Fearon, F. W. G., Eds.; Advances in Chemistry Series 224; American Chemical Society: Washington, DC, 1989. (b) Senshu, K.; Furuzono, T.; Koshizaki, N. *Macromolecules* **1997**, *30*, 4421−4428. (d) Nguyen, P.; Gómez-Elipe, P.; Manners, I. *Chem. Rev.* **1999**, *99*, 1515−1548. (e) Manners, I. *Angew. Chem., Intl. Ed. Engl* **1996**, *35*, 1602−1621. (f) Prange, R.; Allcock, H. R. *Macromolecules* **1999**, *32*, 6390−6392.

(13) (a) Tzeng, F.-Y.; Lin, M.-C.; Wu, J.-Y.; Kuo, J.-C.; Tsai, J.-C.; Hsiao, M.-S.; Chen, H.-L.; Cheng, S. Z. D. *Macromolecules* **2009**, *42*, 3073−3085. (b) Kuo, J.-C.; Lin, W.-F.; Yu, C.-H.; Tsai, J.-C.; Wang, T.-C.; Chung, T.-M.; Ho, R.-M. *Macromolecules* **2008**, *41*, 7967−7977. (c) Tsai, J.-C.; Kuo, J.-C.; Ho, R.-M.; Chung, T.-M. *Macromolecules* **2006**, *39*, 7520−7526. (d) Hsiao, T.-J.; Lee, J.-Y.; Mao, Y.-C.; Chen, Y.-C.; Tsai, J.-C.; Lin, S.-C.; Ho., R.-M. *Macromolecules* **2011**, *44*, 286−298. (e) Ho, R.-M.; Chung, T.-M.; Tsai, J.-C.; Kuo, J.-C.; Hsiao, B. S.; Sics, I. *Macromol. Rapid Commun.* **2005**, *26*, 107−111. (f) Lin, W.-F.; Hsiao, T.-J.; Tsai, J.-C.; Chung, T.-M.; Ho, R.-M. *J. Polym. Sci., Part A: Polym. Chem.* **2008**, *46*, 4843−4856. (g) Lee, J.-Y.; Tsai, J.-C. *J. Polym. Sci., Part A: Polym. Chem.* **2011**, *49*, 3739−3750.

(14) (a) Wolf, F. K.; Hofmann, A. M.; Frey, H. *Macromolecules* **2010**, *43*, 3314−3324. (b) Fu, J.; Luan, B.; Yu, X.; Cong, Y.; Li, J.; Pan, C. Y.; Han, Y. C.; Yang, Y. M.; Li, B. Y. *Macromolecules* **2004**, *37*, 976−986.

(15) (a) Ho, R.-M.; Chen, C.-K.; Chiang, Y.-W. *Macromol. Rapid Commun.* **2009**, *30*, 1439−1456. (b) Tseng, W.-H.; Chen, C.-K.; Chiang, Y.-W.; Ho, R. M.; Akasaka, S.; Hasegawa, H. *J. Am. Chem. Soc.* **2009**, *131*, 1356−1357. (c) Chiang, Y.-W.; Ho., R.-M.; Thomas, E. L.; Burger, C.; Hsiao, B. S. *Adv. Funct. Mater.* **2009**, *19*, 448−459. (d) Chung, T.-M.; Ho, R.-M.; Kuo, J.-C.; Tsai, J.-C.; Hsiao, B. S.; Sics, I. *Macromolecules* **2006**, *39*, 2739−2742.

(16) Natta, G.; Mazzanti, G.; Longi, P.; Bernardini, F. *J. Polym. Sci.* **1958**, *31*, 181−183.

(17) (a) Zeigler, R.; Resconi, L.; Balbontin, G.; Guerra, G.; Venditto, V.; Rose, C. D. *Polymer* **1994**, *35*, 4648−4655. (b) Habaue, S.; Baraki, H.; Okamoto, Y. *Macromol. Chem. Phys.* **1998**, *199*, 2211−2215.

(18) (a) Yasuda, H.; Ihara, E. *Macromol. Chem. Phys.* **1995**, *196*, 2417−2441. (b) Desurmont, G.; Li, Y.; Yasuda, H.; Maruo, T.; Kanehisa, N.; Kai, Y. *Organometallics* **2000**, *19*, 1811−1813. (c) Kawabe, M.; Murata, M. *Macromol. Chem. Phys.* **2001**, *202*, 1799−1805. (d) Kawabe, M.; Murata, M. *Macromol. Chem. Phys.* **2002**, *203*, 24−30. (e) Kaita, S.; Hou, Z.; Wakatsuki, Y. *Macromolecules* **2001**, *34*, 1539−1541. (f) Cai, Z.; Shinzawa, M.; Nakayama, Y.; Shiono, T. *Macromolecules* **2009**, *42*, 7642−7643. (g) Ban, H. T.; Kase, T.; Kawabe, M.; Miyazawa, A.; Ishihara, T.; Hagihara, H.; Tsunogae, Y.; Murata, M.; Shiono, T. *Macromolecules* **2006**, *39*, 171−176. (h) Mason, A. F.; Coates, G. W. *J. Am. Chem. Soc.* **2004**, *126*, 16326−16327. (i) Ruokolainen, J.; Mezzenga, R.; Fredrickson, G. H.; Kramer, E. J. *Macromolecules* **2005**,

38, 851−860. (j) Frauenrath, H.; Balk, S.; Keul, H.; Höcker., H. *Macromol. Rapid Commun.* **2001**, *22*, 1147−1151. (k) Chen, E. Y.-X. *Chem. Rev.* **2009**, *109*, 5157−5214.
(19) (a) Satoh, K.; Kamigaito, M. *Chem. Rev.* **2009**, *109*, 5120−5156. (b) Lutz, J. F.; Jakubowski, W.; Matyjaszewski, K. *Macromol. Rapid Commun.* **2004**, *25*, 486−492. (c) Kamigaito, M.; Satoh, K. *Macromolecules* **2008**, *41*, 269−276.
(20) (a) Chung, T. C. *Prog. Polym. Sci.* **2002**, *27*, 39−85. (b) Atiqullah, M.; Tinkl, M.; Pfaendner, R.; Akhtar, M. N.; Hussain, I. *Polym. Rev.* **2010**, *50*, 178−230.
(21) (a) Razavi, A.; Ferrara, J. *J. Organomet. Chem.* **1992**, *435*, 299−310. (b) Resconi, L.; Piemontesi, F.; Gamurati, I.; Sudmeijer, O.; Nifant'ev, I. E.; Ivchenko, P. V.; Kuz'mina, L. G. *J. Am. Chem. Soc.* **1998**, *120*, 2308−2321.
(22) Patsidis, K.; Alt, G. H.; Milius, W.; Palackal, S. J. *J. Organomet. Chem.* **1996**, *509*, 63−71.
(23) Bochmann, M.; Lancaster, S. J. *Organometallics* **1993**, *12*, 633−640.
(24) Cheng, G.-L.; Hu, C.-P.; Ying, S. K. *Macromol. Rapid Commun.* **1999**, *20*, 303−307.
(25) (a) Amin, S. B.; Marks, T. J. *J. Am. Chem. Soc.* **2007**, *129*, 2938−2953. (b) Carvill, A.; Tritto, I.; Locatelli, P.; Sacchi, M. C. *Macromolecules* **1997**, *30*, 7056−7062. (c) Carvill, A.; Zetta, L.; Zannoni, G.; Sacchi, M. C. *Macromolecules* **1998**, *31*, 3783−3789. (d) Lieber, S.; Brintzinger, H. H. *Macromolecules* **2000**, *33*, 9192−9199. (e) Tynys, A.; Eilertsen, J. L.; Seppala, J. V.; Rytter, E. *J. Polym. Sci., Part A: Polym. Chem.* **2007**, *45*, 1364−1376. (f) Kim, I.; Zhou, J. M. *J. Polym. Sci., Part A: Polym. Chem.* **1999**, *37*, 1071−1082. (g) Kim, I.; Choi, C. S. *J. Polym. Sci., Part A: Polym. Chem.* **1999**, *37*, 1523−1539. (h) Kawahara, N.; Kojoh, S.; Matsuo, S.; Kaneko, H.; Matsugi, T.; Toda, Y.; Mizuna, A.; Kashiwa, N. *Polymer* **2004**, *45*, 2883−2888. (i) Naga, N.; Mizunuma, K. *Polymer* **1998**, *39*, 5059−5067. (h) Naga, N.; Mizunuma, K. *Polymer* **1998**, *39*, 5059−5067. (j) Franceschini, F. C.; Tavares, T. T.; dos Santos, J. H. Z.; Ferreira, M. L.; Soares, J. B.P. *Macromol. Mater. Eng.* **2006**, *291*, 279−287. (k) Franceschini, F. C.; Tavares, T. T.; Greco, P. P.; Galland, G. B.; dos Santos, J. H. Z.; Soares, J. B.P. *J. Appl. Polym. Sci.* **2005**, *95*, 1050−1055.
(26) Han, C. J.; Lee, M. S.; Byun, D. J.; Kim, S. Y. *Macromolecules* **2002**, *35*, 8923−8925.
(27) (a) Resconi, L.; Piemontesi, F.; Franciscono, G.; Abis, L.; Fiorani, T. *J. Am. Chem. Soc.* **1992**, *114*, 1025−1032. (b) Liu, Z.; Somsook, E.; White, C. B.; Rosaaen, K. A.; Landis, C. R. *J. Am. Chem. Soc.* **2001**, *123*, 11193−11207.
(28) (a) Lynd, N. A.; Hillmyer, M. A. *Macromolecules* **2005**, *38*, 8803−8810. (b) Lynd, N. A.; Hillmyer, M. A. *Macromolecules* **2007**, *40*, 8050−8055. (c) Lynd, N. A.; Meuler, A. J.; Hillmyer, M. A. *Prog. Polym. Sci.* **2008**, *33*, 875−893.
(29) Hu, Y.; Krejchi, M. T.; Shah, C. D.; Myers, C. L.; Waymouth, R. M. *Macromolecules* **1998**, *31*, 6908−6916.